Design of VQ-Based Hybrid Digital-Analog Joint Source-Channel Codes for Image Communication*

Yadong Wang, Fady Alajaji and Tamás Linder

Department of Mathematics and Statistics
Queen's University, Kingston, Ontario, Canada K7L 3N6

Abstract

A joint source-channel coding system for image communication over an additive white Gaussian noise channel is presented. It employs vector quantization based hybrid digital-analog modulation techniques with bandwidth compression and expansion for transmitting and reconstructing the wavelet coefficients of an image. The main advantage of the proposed system is that it achieves good performance at the design channel signal-to-noise ratio (CSNR), while still maintaining a "graceful improvement" characteristic at higher CSNRs. Comparisons are made with two purely digital systems and two purely analog systems. Simulation shows that the proposed system is superior to the other investigated systems for a wide range of CSNRs.

Index Terms: Hybrid digital-analog coding, joint source-channel coding, vector quantization, broadcasting, robustness, image coding, discrete wavelet transform.

1 Introduction

In applications such as broadcasting and robust communication of analog-valued sources over wireless channels, there is a large variation in channel conditions depending on the physical landscape, the communication distance, the weather situation, etc. Thus, a communication system designed to perform well for a broad range of channel conditions is highly desired. Since it is difficult to introduce efficient signal compression in purely analog communication schemes, digital communication techniques are often preferred. One of the main advantages of digital communication over analog communication is that it can be designed to (asymptotically) achieve the theoretically optimal performance for a fixed channel signal-to-noise ratio (CSNR). This excellent performance can be achieved by the separate design of optimal source and channel codes. Systems which are designed based on this principle are often referred to as *tandem source-channel coding* systems. There are, however, two fundamental disadvantages associated with digital tandem systems. One is the *threshold*

*This work was supported in part by NSERC of Canada and PREA of Ontario. Authors E-mail: {yadong, fady, linder}@mast.queensu.ca.

effect: the system typically performs well at the design CSNR, while it degrades drastically when the true CSNR falls beneath the design CSNR. This effect is due to the quantizer's sensitivity to channel errors and the total breakdown of most powerful error-correcting codes at low CSNRs. The other trait is the *levelling-off effect*: as the CSNR increases, the performance remains constant beyond a certain threshold. This problem is due to the non-recoverable distortion introduced by the quantizer which limits the system performance at high CSNRs.

To cope with the first problem, various digital systems known as *joint source-channel* (JSC) coding systems have been proposed. By jointly designing the source and channel codes, many results (e.g., [6]-[10]) show that noticeable gain can be obtained in terms of coding efficiency, reconstructed signal quality, coding delay and complexity. In particular, JSC schemes are more robust than tandem systems at low CSNRs. However both coding systems still suffer from the levelling-off effect at high CSNRs, since being digital systems, they employ quantization to "digitize" the source. On the other hand, analog systems do not suffer from the levelling-off effect, although they are generally inferior to digital systems in terms of rate-distortion-capacity performance, particularly at the design CSNR.

In [1], Mittal and Phamdo propose a class of hybrid digital-analog (HDA) JSC coding systems. They show that HDA systems can asymptotically achieve the optimal performance at the design CSNR, while maintaining a "graceful improvement" at high CSNRs. The threshold effect, although still inherent, is also less severe. Thus, HDA systems exploit the advantages of both digital and analog systems. In [2], an application of an HDA system to the coding of speech signals over Gaussian channels is presented. In [3], Skoglund, Phamdo and Alajaji introduce and implement a vector quantization (VQ) based HDA system with linear mapping in its analog component. They also optimize the HDA system parameters using a similar procedure to that of channel optimized vector quantization, hence increasing the system's error resilience at low CSNRs. The system in [3] is valid only for bandwidth expansion. In [4, 5], a VQ based HDA system for both bandwidth expansion and bandwidth compression is investigated. It employs a Karhunen-Loéve transform to decorrelate the source, Turbo error-correcting coding in its digital part to improve the system performance at low CSNRs and superposition coding of the analog and digital signals. This system also allows for both linear and non-linear mapping in its analog component. Other methods which combine digital and analog coding techniques include [11]-[16].

In this paper, we present an HDA image communication scheme for additive white Gaussian noise (AWGN) channels. Our main objective is to design a simple (low-complexity, low-delay) system which performs well over a wide range of channel CSNRs, with the same emphasis as in [1]-[5] of obtaining a "graceful improvement" characteristic at high CSNRs. This characteristic is particularly appealing for Telemedicine and sensor networks applications where sensitive image data need to be reliably communicated from remote locations irrespective of the channel environment. Section 2 gives a brief introduction to the HDA systems. In Section 3, the proposed image coding scheme is presented. Simulation results are given in Section 4, and comparisons are made with purely digital and purely analog systems. Finally, Section 5 concludes the paper.

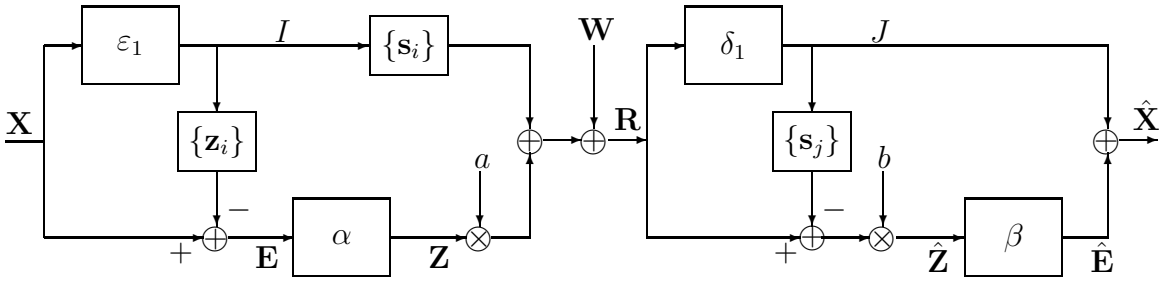

Figure 1: HDA system for bandwidth compression/expansion.

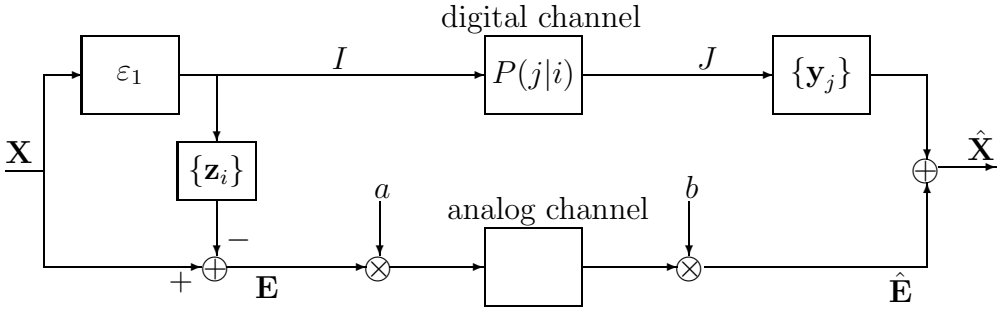

Figure 2: HDA system for bandwidth expansion.

2 HDA System Description

We consider the problem of transmitting a d-dimensional analog source vector $\mathbf{X} \in \mathbb{R}^d$ over a memoryless Gaussian channel and reproducing it as $\hat{\mathbf{X}}$ at the receiver. In Fig. 1, we present a general HDA system for bandwidth compression/expansion. The system is a simplified version of the system presented in [4, 5], as it does not employ error correcting codes in the digital part to avoid incurring additional delay and complexity. In the digital part, the output index I of the VQ encoder ε_1 is assigned a $\tilde{d}$-dimensional channel symbol $\mathbf{s}_I$ from a finite set $\{\mathbf{s}_i\}$ of possible symbols. The index I also chooses a vector $\mathbf{z}_I$ from the *encoder codebook* $\{\mathbf{z}_i\}$. The vector $\mathbf{z}_I$ is subtracted from $\mathbf{X}$ to form the (quantization) error vector $\mathbf{E}$, and this vector is then used as input to the mapping α, with output $\mathbf{Z} = \alpha(\mathbf{E}) \in \mathbb{R}^{\tilde{d}}$. The scaled version, $a \cdot \mathbf{Z}$, is added to $\mathbf{s}_I$ and then fed to a discrete-time *analog-amplitude* channel with AWGN of zero mean and variance σ^2 per component. The scaling constant a regulates the power allocation of the analog part with respect to the overall channel input power.

At the receiver, the received vector $\mathbf{R}$ is first fed to decoder δ_1, resulting in output index J, and a reconstructed codevector $\mathbf{y}_J$ is chosen for the digital part. Meanwhile, the output index J is assigned a channel symbol. The result is subtracted from the received vector $\mathbf{R}$ and scaled by the constant b, forming an estimate $\hat{\mathbf{Z}}$. This estimate is then fed to the analog mapping β, and the output $\hat{\mathbf{E}}$ is added to $\mathbf{y}_J$ of the digital part, resulting in the source vector estimate $\hat{\mathbf{X}}$.

In Fig. 2, we depict the HDA system for bandwidth expansion investigated in

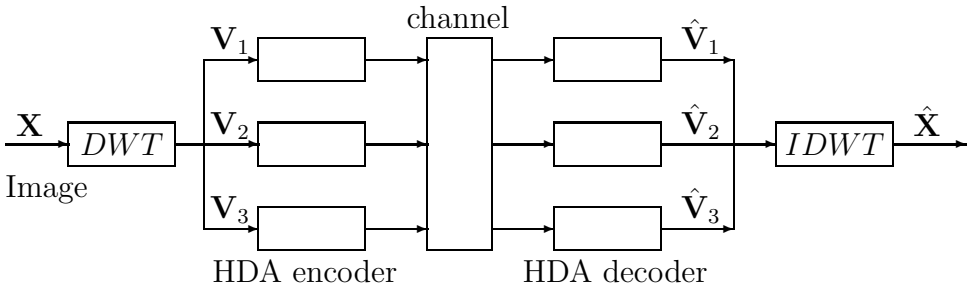

Figure 3: The structure of the HDA image coding system.

[3]. Note however that this system is a special case of the above bandwidth compression/expansion system [4, 5]. Indeed, in the bandwidth compression/expansion system, if we choose the channel symbols of the digital part as $(\mathbf{s}_i, \mathbf{0})^T$, and choose the mapping α as $\alpha(\mathbf{E}) = (\mathbf{0}, \mathbf{E})^T$, then Fig. 1 reduces to Fig. 2.

3 Image Coding Schemes

We consider the problem of transmitting gray-scale still images over a memoryless Gaussian channel. Our design will focus on obtaining a good overall performance with a "graceful improvement" characteristic at high CSNRs.

3.1 Vector Structures

Fig. 3 shows the block diagram of the proposed image coding system. An image is first decomposed using a two-dimensional separable discrete wavelet transform (DWT); here Antonni 9/7 biorthorgonal filters are used for DWT. The DWT is applied three times, each time on the lowest frequency subband of the previous resolution level, resulting in 10 subbands overall. The variance and mean of each subband are estimated and all the wavelet coefficients are normalized to have zero mean and unit variance. The normalized coefficients are grouped into vectors as follows.

- For the lowest frequency subband (LFS), each block of 2×2 coefficients form a vector of dimension 4, and referred to as a class 1 vector.
- For the highest frequency levels (there are three such subbands in total), each block of 4×4 coefficients form a vector of dimension 16, and referred to as a class 3 vector.
- For the remaining two frequency levels (six subbands in total with three subbands for each level), one coefficient from the coarser level and a block of 2×2 coefficients from the finer level (with the same frequency direction as the coarser one) form a vector of dimension 5, and referred to as a class 2 vector.

Since the three classes of vectors have unequal roles in the reconstruction of the overall image, different coding strategies will be employed in their processing and transmission.

3.2 Bandwidth Expansion

In [3], an iterative training algorithm is presented to find the optimal design of the HDA system for bandwidth expansion. Here, we use the system in [3] with a transmission rate of 2 channel uses/source symbol to code vectors of class 1 and class 2, since these classes of vectors involve the low and middle frequency components of the image, which are vital for the overall image quality. In total, 1/4 of the coefficients are coded using the bandwidth expansion system.

3.3 Bandwidth Compression

The remaining 3/4 portion of the coefficients is formed into vectors of class 3 and coded via the HDA bandwidth compression system. In particular, we employ an HDA system with a rate of 1/2 channel use/source symbol. The system is realized as follows. For a d-dimensional analog vector source (here for class 3 vectors, $d = 16$), a VQ of $d/2$ bits is employed. The mapping α in the analog part takes in a d-dimensional error vector $\mathbf{E}$ and outputs a vector $\mathbf{Z}$ of dimension $d/2$. More precisely, $\mathbf{E}$ is decomposed into $d/2$ two-dimensional subvectors (components 1 and 2 in the first vectors, 3 and 4 in second, etc.), and for each subvector, an output is generated using the arithmetic average value of the two components. Similarly, the decoding mapping β reconstructs each two-dimensional subvector using the corresponding component of $\hat{\mathbf{Z}}$, to form the estimate $\hat{\mathbf{E}}$.

By adopting the approach in [3], we optimize (in the sense of minimizing the overall mean square error distortion) the above compression system as follows. For an arbitrary vector $\mathbf{X} \in \mathbb{R}^d$, denote $\mathbf{X}^1 = (X_1, X_3, \ldots, X_{d-1})^T$, $\mathbf{X}^2 = (X_2, X_4, \ldots, X_d)^T$ and $\bar{\mathbf{X}} = \mathbf{X}^1 + \mathbf{X}^2$. For a fixed encoder ε_1, it can be shown that the optimal $\{\mathbf{z}_i\}$, $\{\mathbf{y}_j\}$ and b are given by

$$\mathbf{z}_i^k = \mathbf{m}_y^k(i) + b(\mathbf{s}_i - \mathbf{m}_s(i)), \quad k = 1, 2, \quad i = 0, \ldots, N-1, \tag{1}$$

$$\mathbf{y}_j^k = E[\mathbf{X}^k - \frac{1}{2}ab(\bar{\mathbf{X}} - \bar{\mathbf{z}}_I) - b(\mathbf{s}_I - \mathbf{s}_J + \mathbf{W})|J = j], \tag{2}$$

$$b = \frac{E\left[\bar{\mathbf{X}}^T(\frac{a}{2}(\bar{\mathbf{X}} - \bar{\mathbf{z}}_I - E[\bar{\mathbf{X}} - \bar{\mathbf{z}}_I|J]) + \mathbf{s}_I - E[\mathbf{s}_I|J])\right]}{2E||\frac{a}{2}(\bar{\mathbf{X}} - \bar{\mathbf{z}}_I - E[\bar{\mathbf{X}} - \bar{\mathbf{z}}_I|J]) + \mathbf{s}_I - E[\mathbf{s}_I|J]||^2 + \sigma^2 d}, \tag{3}$$

where $N = 2^{\frac{d}{2}}$, $\bar{\mathbf{m}}_y^k(i) = E[\bar{\mathbf{y}}_J|I = i]$ and $\mathbf{m}_s(i) = E[\mathbf{s}_J|I = i]$. Furthermore, for a fixed decoder δ_1, the optimal encoder regions are

$$\begin{aligned} \mathbb{S}_i = \Big\{ & x \in \mathbb{R}^d : ||\mathbf{x} - \mathbf{z}_i||^2 + \left(\frac{1}{2}a^2b^2 - ab\right)||\bar{\mathbf{x}} - \bar{\mathbf{z}}_i||^2 + h_i \\ & \leq ||\mathbf{x}^k - \mathbf{z}_j^k||^2 + \left(\frac{1}{2}a^2b^2 - ab\right)||\bar{\mathbf{x}} - \bar{\mathbf{z}}_j||^2 + h_j, \forall j \Big\}, \end{aligned} \tag{4}$$

where

$$h_i \stackrel{\triangle}{=} \sum_{k=1}^{2} E[||\mathbf{y}_J^k + \beta(\mathbf{s}_I - \mathbf{s}_J)||^2 | I = i] - E[||\mathbf{z}_I||^2 | I = i].$$

These optimality results are next utilized (as in [3]) to formulate an iterative training algorithm for the compression system. Although they are derived here for a system with rate 1/2, they can also be determined for an HDA compression system with any rate less than 1.

3.4 Models for Wavelet Coefficients

It is known that the distribution of the wavelet coefficients of each subband can be well approximated by the generalized Gaussian distribution (GGD) (e.g., [17, 18]) whose probability density function (pdf) is given by

$$f(x) = \frac{\alpha\eta(\alpha, \sigma_s)}{2\Gamma(1/\alpha)} \exp\{-[\eta(\alpha, \sigma_s)|x|]^\alpha\}$$

where $\eta(\alpha, \sigma_s) = \frac{1}{\sigma_s}\left(\frac{\Gamma(3/\alpha)}{\Gamma(1/\alpha)}\right)^{\frac{1}{2}}$, $\alpha > 0$ is a shaping parameter, σ_s is the standard deviation of the distribution, and $\Gamma(\cdot)$ is the Gamma function. The pdf of the GGD reduces to the Laplacian pdf when $\alpha = 1$ and yields the Gaussian pdf when $\alpha = 2$. Based on our experiments on natural images and the results in [17], we assume a Laplacian distribution for all subbands. All coefficients are quantized using a VQ trained for a Laplacian source with zero mean and unit variance.

3.5 Adaptive Decoding

As in [3], motivated by a broadcast scenario, we apply the training algorithms to a fixed-encoder adaptive-decoder optimized HDA system. For example, the optimized HDA bandwidth expansion system is designed for a fixed CSNR value $*$ (in decibels), yielding a fixed encoder ε_1, and fixed $\{\mathbf{z}_i\}$ and a, which are not modified as the true CSNR changes. On the other hand, the decoder has knowledge of the true CSNR and adapt to it by updating the values of $\{\mathbf{y}_j\}$ and b as the CSNR varies.

3.6 Side Information

Certain side information must be reliably transmitted over the channel, including the means and variances of each subband. By observing the statistical properties of the subband data for a variety of images, we found that the mean values for all subbands except for the LFS are very small compared to the standard deviation. Thus, all these mean values (except the LFS) are assumed to be zero in our design. For a 3-level 10-band octave decomposition, we use 12 bits to quantize the variance of each subband and 8 bit to quantize the mean value of the LFS, resulting in a total of 128 bits. The image size needs to also be known at the receiver (it is represented via a natural binary code). The side information is usually error protected before

transmission. For an image of size 512×512 and a rate-1/2 error control code, the overhead consists of 292 bits in total, or equivalently around 0.001 bits per pixel. In the following discussion, we assume that the side information is transmitted error free, and we do not include it in the calculation of the overall system rate (as it is negligible).

4 Simulation Results

We next implement the proposed HDA image coding system for the transmission of gray-scale images over AWGN channels and test it for the images Lena and Goldhill, both of size 512×512. Binary phase-shift keying (BPSK) modulation is used in the digital part of the HDA system. Performance comparisons are made with purely analog and purely digital systems.

A. VQHDA System

In the VQHDA system, 5-bit and 4-bit VQs are used to quantize class 1 and class 2 vectors, respectively. The codebooks are trained using the corresponding training algorithm for the rate-2 bandwidth expansion HDA system. An 8-bit VQ is employed to quantize class 3 vectors. The codebooks are obtained using the training algorithm for the rate-$\frac{1}{2}$ compression HDA system. All VQs are trained using 300,000 training vectors. The encoder of each VQ is determined for a fixed CSNR, while adaptive decoding is employed at the receiver. The overall channel input power is set to unity in all systems. For bandwidth compression, 10% of the total power is allocated to the analog part, while for bandwidth expansion the power is evenly distributed between the digital and analog parts (the best power allocation between the digital and analog parts is determined via a numerical study). The overall system rate is 0.83 channel use/pixel. For comparison, we also evaluate the performance of one purely analog system and two purely digital systems.

B. Purely Analog System

The purely analog system, denoted by Analog, consists of a rate-one linear analog code (α, β), where $\alpha : \mathbb{R}^d \to \mathbb{R}^d$ is a linear encoder and $\beta : \mathbb{R}^d \to \mathbb{R}^d$ is a linear decoder. Let the source variance be σ_s^2 and the channel input power constraint be P (which is set to unity in the simulations), while the channel noise variance is σ^2. The encoder/decoder pair is given by

$$\alpha(\mathbf{X}) = \sqrt{\frac{P}{\sigma_s^2}}\mathbf{X} \qquad \text{and} \qquad \beta(\mathbf{Z}) = \frac{\sqrt{\sigma_s^2 P}}{P + \sigma^2}\mathbf{Z}.$$

Note that the encoder α is independent of the noise variance σ^2. The system employs a similar rate allocation as that of the VQHDA system. Class 1 and class 2 vectors are transmitted twice, and the receiver employs a linear minimum mean square error decoder. Class 3 vectors employ a similar method as in the bandwidth compression system, taking 2 components as input and sending the average value. The total rate of the system is around 0.875 channel use/pixel.

C. Purely Digital System

Two purely digital systems are also investigated. The first digital system uses channel optimized vector quantization (COVQ). For this system, vectors are formed using the same vector schemes as in the VQHDA system. A 4-dimensional 9-bit COVQ, a 5-dimensional 9-bit COVQ, and a 16-dimensional 8-bit COVQ are trained at a designed CSNR using 100,000 training vectors. The output indices of each VQ are then directly sent over the BPSK modulated channel. The channel input power per channel use is also set to unity. The receiver employs hard decision demodulation and adaptive COVQ decoding. The second digital system, denoted by LBG-VQ, uses the Linde, Buzo and Gray (LBG) vector quantization algorithm, where a 4-dimensional 9-bit LBG-VQ, a 5-dimensional 9-bit LBG-VQ, and a 16-dimensional 8-bit LBG-VQ are trained using 300,000 training vectors. The remaining system parts are identical to their counterparts in the COVQ system. Adaptive decoding is also employed. Both systems have an overall rate of 0.832 channel use/pixel.

D. Results

The performance of each system is measured in terms of the peak signal-to noise ratio (PSNR), which is defined (in dB) by

$$\text{PSNR} = 10 \log_{10} \frac{(255)^2}{D},$$

where D is the mean square error between the original and decoded images. In Figs. 4 and 5, we present performance results for the various systems, where the encoder of both the proposed VQHDA system and the COVQ system is designed for a fixed CSNR of 10 dB. We observe that the VQHDA system outperforms the purely analog and LBG-VQ systems for most CSNRs, and provide substantial improvements over the purely digital systems from medium to high CSNRs. Note that the performance of the VQHDA system saturates at a CSNR of 30 dB; this is due to the non-reversible analog linear map in the bandwidth compression system. It is observed in [4] that replacing the linear analog map with a non-linear map enables the HDA system to saturate at an arbitrarily high CSNR.

5 Conclusion

An image communication system using VQ-based HDA JSC coding for AWGN channels is proposed. Both bandwidth expansion and compression HDA systems are used for the coding and transmission of the image wavelet coefficients: bandwidth expansion is applied on the low and medium frequency subbands, while bandwidth compression is applied on the high frequency subbands. Numerical results show that the proposed system is superior to purely analog and purely digital systems for a wide range of CSNRs. The power and rate allocations in the proposed scheme are selected via a numerical study. Future work may focus on optimizing the rate allocation among the different subbands, optimizing the power allocation between the digital and analog parts, and applying non-linear analog maps for the bandwidth compression system.

References

[1] U. Mittal and N. Phamdo, "Hybrid digital-analog (HDA) joint source-channel codes for broadcasting and robust communications," *IEEE Trans. Inform. Theory*, vol. 48, May 2002.

[2] N. Phamdo and U. Mittal, "A joint source-channel speech coder using hybrid digital-analog (HDA) modulation," *IEEE Trans. Speech and Audio Processing*, vol. 10, no. 4, May 2002.

[3] M. Skoglund, N. Phamdo and F. Alajaji, "Design and performance of VQ-based hybrid digital-analog joint source-channel codes," *IEEE Trans. Inform. Theory*, vol. 48, no. 3, March 2002.

[4] M. Skoglund, N. Phamdo and F. Alajaji, "Hybrid digital-analog coding for bandwidth compression/expansion using VQ and Turbo codes," in *Proc. IEEE Int. Symp. Inform. Theory*, Washington, DC, June, 2001, p. 260.

[5] M. Skoglund, N. Phamdo and F. Alajaji, "Hybrid digital-analog source-channel coding for bandwidth compression and expansion systems," *preprint*, to be submitted.

[6] H. Kumazawa, M. Kasahara and T. Namekawa, "A construction of vector quantizers for noisy channels," *Electronics and Engineering in Japan,* vol. 67-B, pp. 39-47, Jan. 1984.

[7] E. Ayanoglu and R. M. Gray, "The design of joint source and channel trellis waveform coders," *IEEE Trans. Inform. Theory,* vol. 33, pp. 855-865, Nov. 1987.

[8] K. A. Zeger and A. Gersho, "Pseudo-Gray coding," *IEEE Trans. Communications*, vol. 38, pp. 2147-2158, Dec. 1990.

[9] N. Farvardin and V. Vaishampayan, "On the performance and complexity of channel-optimized vector quantizers," *IEEE Trans. Inform. Theory*, vol. 37, pp. 155-159, Jan. 1991.

[10] J. Lim and D. L. Neuhoff, "Joint and tandem source-channel coding with complexity and delay constraints," *IEEE Trans. Commun.*, vol. 51, pp. 757-766, May 2003.

[11] J. M. Lervik, A. Grovlen and T. A. Ramstad, "Robust digital signal compression and modulation exploiting the advantages of analog communications," in *Proc. IEEE GLOBECOM*, Singapore, Nov. 1995, pp. 1044-1048.

[12] A. Fuldseth and T. A. Ramstad, "Bandwidth compression for continuous amplitude channels based on vector approximation to a continuous subset of the source signal space," in *Proc. IEEE Int. Conf. Acoustics, Speech, Signal Processing*, Munich, Germany, April 1997, pp. 3093-3096.

[13] I. Kozintsev and K. Ramchandran, "Hybrid compressed–uncompressed framework for wireless image transmission," in *Proc. IEEE Int. Conf. Commun.*, Montréal, June 1997, pp. 77-80.

[14] S. Shamai, S. Verdú and R. Zamir, "Systematic lossy source/channel coding," *IEEE Trans. Inform. Theory*, vol. 44, no. 2, March 1998.

[15] H. Coward and T. A. Ramstad, "Quantizer optimization in hybrid digital-analog transmission of analog source signals," in *Proc. IEEE Int. Conf. Acoustics, Speech, Signal Processing*, 2000.

[16] H. Coward and T. A. Ramstad, "Robust image communication using bandwidth reducing and expanding mappings," in *Proc. 34th Asilomar Conf. Signals, Systems, and Computers*, Pacific Grove, CA, USA, Oct. 29- Nov. 1, 2000.

[17] N. Tanabe and N. Farvardin, "Subband image coding using entropy-coded quantization over noisy channels," *IEEE J. Select. Areas Commu.*, vol. 10 , pp. 926-943, June 1992.

[18] P. Hedelin and J. Skoglund, "Vector quantization based on Gaussian mixture models," *IEEE Trans. Speech Audio Processing*, vol. 8, pp. 385-401, July 2000.

COVQ, PSNR=28.24 dB Analog, PSNR=27.18 dB VQHDA, PSNR=33.69 dB

COVQ, PSNR=28.37 dB Analog, PSNR=33.58 dB VQHDA, PSNR=37.03 dB

Figure 4: Comparison between the different systems, where the VQHDA and COVQ systems are designed at CSNR = 10 dB . The true CSNR is 10 dB for the first row and 20 dB for the second row. Adaptive decoding is used for all systems.

Lena 512×512	True CSNR (in dB)						
	0	5	10	15	20	25	30
VQHDA at 10 dB	17.53	23.15	33.41	37.67	39.61	40.80	41.01
Analog	18.71	22.54	27.16	31.57	35.14	37.54	39.16
COVQ at 10 dB	18.48	25.19	28.24	28.27	28.27	28.27	28.27
LBG-VQ	14.76	17.46	27.20	28.29	28.34	28.34	28.34

Goldhill 512×512	True CSNR (in dB)						
	0	5	10	15	20	25	30
VQHDA at 10 dB	16.76	22.02	32.06	35.37	37.00	37.75	38.03
Analog	18.28	21.99	26.41	30.45	33.50	35.15	36.44
COVQ at 10 dB	18.10	25.13	28.35	28.37	28.37	28.37	28.37
LBG-VQ	14.51	17.17	27.36	28.46	28.48	28.48	28.48

Figure 5: PSNR results for the different systems for transmitting Lena 512×512 and Godlhill 512×512 with rate 0.83 channel use/pixel (except the analog system with rate 0.875 channel use/pixel). Adaptive decoding is employed in all systems.